Task Accuracy Measure based on Dynamic Process for Cooperating Manipulation System

Tasuku YAMAWAKI and Masahito YASHIMA
Dept. of Mechanical Systems Engineering
National Defense Academy of Japan
Hashirimizu, Yokosuka 239-8686, JAPAN
{yamawaki, yashima}@nda.ac.jp

***Abstract*— The present paper introduces an evaluation of the manipulation performance of a cooperating robotic manipulator with respect to task accuracy, taking into consideration the effects of the dynamic process between inputs and outputs in the manipulation system. A measure based on the output controllability of the manipulation system is proposed, which shows the relationship between the object's position and orientation and the joint driving force. Computer simulations show the validity of the task accuracy measure and the difference between the proposed measure and the conventional manipulability measure.**

I. INTORDUCTION

The concepts of kinematic manipulability measure and dynamic manipulability measure were proposed for evaluation of kinematic and dynamic performance for a single manipulator in a task space [17], [18]. Performance criteria related to the manipulability are the generalized inertia ellipsoid [1], the task compatibility [5], the acceleration radius [7] and the dynamic isotropy conditions [11]. The basic idea of the manipulability measure has been applied to cooperating manipulation systems, which consists of multiple robotic manipulators and a grasped object [2], [3], [4].

Typical task examples of cooperating robotic manipulators are manipulating an object from one position and orientation to another, or are mating mechanical parts in gravitational fields. In such a manipulation task, control accuracy of the object's position and orientation is important issues. The above-mentioned manipulability measures, however, take into consideration not the task accuracy but the task efficiency for given joint velocities or joint driving forces. In this paper, we consider the task accuracy of the cooperating manipulation system as manipulation performance.

From the viewpoint of the linear system theory [9], the relationship between inputs and outputs in the cooperating manipulation system shown in Fig.1 is discussed. A system is said to be a static process when the current output is determined only by the current input at the moment. The conventional kinematic (dynamic) manipulability is regarded as the measure of the static process, since the relationship between joint velocities (torques) and arm tip velocities (accelerations) is considered to be instantaneous.

On the other hand, a system is said to be a dynamic process when the current output is affected by not only the current inputs but also the past inputs. It is required to take the dynamic process of a system into consideration in order to evaluate the control accuracy of the system [9]. Therefore, considering the dynamic process of the cooperating manipulation system, we discuss the task accuracy of the system from the viewpoint of the output controllability between the object's position and orientation (outputs) and the joint driving forces (inputs).

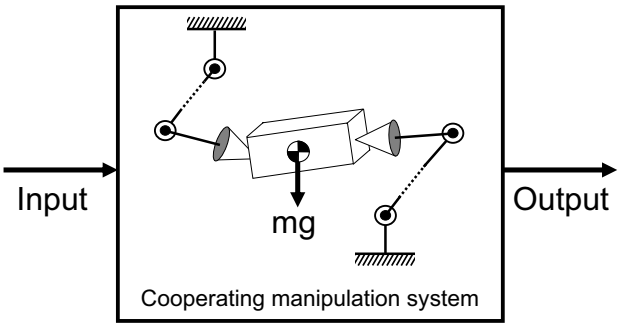

Fig. 1. Concept of dynamic process and static process in cooperating manipulation system

In the present paper, the relationship between inputs and outputs in the cooperating manipulation system is reconsidered from the viewpoint of a dynamic process, and the evaluation for the manipulation performance from the aspect of task accuracy is proposed. We present a novel ellipsoid expressing the set of output controllable displacements of the object in terms of the given joint driving forces, which completely differs from the conventional manipulability ellipsoids. The volume, shape, and orientation of the ellipsoid can yield the performance evaluation of the task accuracy quantitatively. Computer simulations show the validity of the task accuracy measure and the difference between the proposed measure and the conventional manipulability measure.

II. LINEARIZED MODEL

A. Kinematic constraints

A cooperating manipulation system consists of an object and multiple cooperating robot manipulators in the three dimensional space, as shown in Fig. 2. It is assumed that each manipulator has three joints in order to generate forces in an arbitrary direction at each contact point [15]. The object is

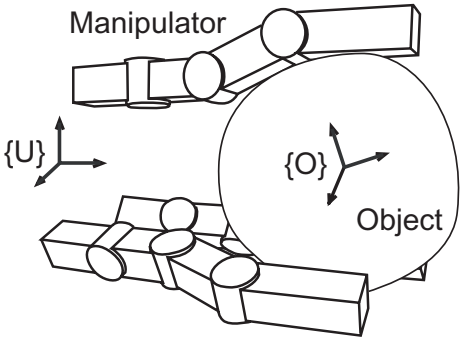

Fig. 2. Cooperating manipulation system

manipulated by multiple rigid manipulators through contacts on the distal link of each manipulator.

Let $\boldsymbol{x}_O \in \Re^6$ denote the position and orientation of the object, whose frame is fixed to the object mass center. Let $\boldsymbol{\theta} \in \Re^{3n_f}$ be the vector of the joint angle of the n_f-manipulators. Assuming that sliding does not occur at any contact points by applying appropriate contact forces, the velocity constraints between $\dot{\boldsymbol{x}}_O$ and $\dot{\boldsymbol{\theta}}$ can be described as

$$\boldsymbol{W}_O^T(\boldsymbol{x}_O, \boldsymbol{\xi})\ \dot{\boldsymbol{x}}_O = \boldsymbol{J}(\boldsymbol{\theta}, \boldsymbol{\xi})\ \dot{\boldsymbol{\theta}} \tag{1}$$

where $\boldsymbol{W}_O = \boldsymbol{T}^T\boldsymbol{W} \in \Re^{6\times 3n_f}$, $\boldsymbol{W}$ is the wrench matrix and $\boldsymbol{T}$ is the matrix that transforms $\dot{\boldsymbol{x}}_O$ into the vector of the linear and angular velocity of the object $(\boldsymbol{v}_O,\ \boldsymbol{\omega}_O)$. The matrix $\boldsymbol{J} \in \Re^{3n_f\times 3n_f}$ is the manipulator Jacobian matrix. The vector $\boldsymbol{\xi} \in \Re^{4n_f}$ is the local coordinate, which represents the position of the contact point on the surface of the object and the link of the manipulator [12].

B. Dynamics of Manipulation System

The equation of motion for the manipulator are given by

$$\boldsymbol{M}_H(\boldsymbol{\theta})\ddot{\boldsymbol{\theta}} + \boldsymbol{h}_H(\boldsymbol{\theta}, \dot{\boldsymbol{\theta}}) + \boldsymbol{g}_H(\boldsymbol{\theta}) = \boldsymbol{\tau} - \boldsymbol{J}^T\boldsymbol{f}_C \tag{2}$$

where $\boldsymbol{M}_H \in \Re^{3n_f\times 3n_f}$ is the inertia matrix, $\boldsymbol{h}_H \in \Re^{3n_f}$, $\boldsymbol{g}_H \in \Re^{3n_f}$, $\boldsymbol{\tau} \in \Re^{3n_f}$ and $\boldsymbol{f}_C \in \Re^{3n_f}$ are the vectors of the Coriolis term, the gravitational term, joint torques, and components of the contact forces exerted by the manipulators at their contact points, respectively.

The equation of motion for the object are described as

$$\boldsymbol{M}_O(\boldsymbol{x}_O)\ddot{\boldsymbol{x}}_O + \boldsymbol{h}_O(\boldsymbol{x}_O, \dot{\boldsymbol{x}}_O) + \boldsymbol{g}_O(\boldsymbol{x}_O) = \boldsymbol{W}(\boldsymbol{x}_O, \boldsymbol{\xi})\boldsymbol{f}_C \tag{3}$$

where $\boldsymbol{M}_O \in \Re^{6\times 6}$ is the inertia matrix of the object, and $\boldsymbol{h}_O \in \Re^6$ and $\boldsymbol{g}_O \in \Re^6$ are the vectors of the Coriolis and gravitational terms, respectively.

The contact forces generating the acceleration of the object can be derived from (3), which are

$$\boldsymbol{f}_C = \boldsymbol{W}^\sharp(\boldsymbol{M}_O\ddot{\boldsymbol{x}}_O + \boldsymbol{h}_O + \boldsymbol{g}_O) + \boldsymbol{N}\boldsymbol{f}_I \tag{4}$$

where $\boldsymbol{W}^\sharp$ is the pseudo inverse of $\boldsymbol{W}$, the vector $\boldsymbol{N}\boldsymbol{f}_I$ represents the internal force, and $\boldsymbol{f}_I \in \Re^{(3n_f-6)}$ denotes its magnitude.

The acceleration constraints are obtained by differentiating the velocity constraint (1). Therefore, the joint angular acceleration $\ddot{\boldsymbol{\theta}}$ can be given by

$$\ddot{\boldsymbol{\theta}} = \boldsymbol{J}^{-1}(\boldsymbol{W}_O^T\ddot{\boldsymbol{x}}_O + \dot{\boldsymbol{W}}_O^T\dot{\boldsymbol{x}}_O - \dot{\boldsymbol{J}}\dot{\boldsymbol{\theta}}) \tag{5}$$

Substituting (4) and (5) into (2) yields the dynamic equations for the whole manipulation system, which are

$$\boldsymbol{M}_{\text{sys}}\begin{bmatrix} \ddot{\boldsymbol{x}}_O \\ \boldsymbol{f}_I \end{bmatrix} = \boldsymbol{\tau} - \boldsymbol{g}_{\text{sys}}(\boldsymbol{x}_O, \boldsymbol{\theta}, \boldsymbol{\xi}) - \boldsymbol{h}_{\text{sys}} \tag{6}$$

where

$$\begin{aligned}
\boldsymbol{M}_{\text{sys}} &= \begin{bmatrix} \boldsymbol{M}_V & \boldsymbol{J}^T\boldsymbol{N} \end{bmatrix} \in \Re^{3n_f\times 3n_f} \\
\boldsymbol{M}_V &= \boldsymbol{M}_H\boldsymbol{J}^{-1}\boldsymbol{W}_O^T + \boldsymbol{J}^T\boldsymbol{W}^\sharp\boldsymbol{M}_O \in \Re^{3n_f\times 6} \\
\boldsymbol{g}_{\text{sys}} &= \boldsymbol{g}_H + \boldsymbol{J}^T\boldsymbol{W}^\sharp\boldsymbol{g}_O \\
\boldsymbol{h}_{\text{sys}} &= \boldsymbol{h}_H + \boldsymbol{J}^T\boldsymbol{W}^\sharp\boldsymbol{h}_O + \boldsymbol{M}_H\boldsymbol{J}^{-1}(\dot{\boldsymbol{W}}_O^T\dot{\boldsymbol{x}}_O - \dot{\boldsymbol{J}}\dot{\boldsymbol{\theta}})
\end{aligned}$$

Solving for $[\ddot{\boldsymbol{x}}_O^T\ \boldsymbol{f}_I^T]^T$ on the left-hand side of (6) yields

$$\ddot{\boldsymbol{x}}_O = \boldsymbol{\Lambda}_O(\boldsymbol{\tau} - \boldsymbol{g}_{\text{sys}} - \boldsymbol{h}_{\text{sys}}) \tag{7}$$

$$\boldsymbol{f}_I = \boldsymbol{\Lambda}_f(\boldsymbol{\tau} - \boldsymbol{g}_{\text{sys}} - \boldsymbol{h}_{\text{sys}}) \tag{8}$$

where

$$\boldsymbol{M}_{\text{sys}}^{-1} = \begin{bmatrix} \boldsymbol{\Lambda}_O \\ \boldsymbol{\Lambda}_f \end{bmatrix}$$

Consequently, the dynamics of the manipulation system can be divided into two properties. Equation (7) represents the relationship between the applied joint torque $\boldsymbol{\tau}$ and the generated acceleration of the object $\ddot{\boldsymbol{x}}_O$, and equation (8) represents the relationship between the applied joint torque $\boldsymbol{\tau}$ and the generated internal force $\boldsymbol{f}_I$.

C. State Equation and Output Equation

By applying the linear system theory, we derive the linearized dynamic model of (7), which shows the relationship between the object's position and orientation and the joint torques.

Linearizing (7) with respect to the equilibrium points $\boldsymbol{x}_O = \boldsymbol{x}_{Oe}$, $\boldsymbol{\theta} = \boldsymbol{\theta}_e$, $\boldsymbol{\xi} = \boldsymbol{\xi}_e$, $\boldsymbol{\tau} = \boldsymbol{\tau}_e$ and $\boldsymbol{p} = \boldsymbol{p}_e$, which satisfy $\ddot{\boldsymbol{x}}_O = \dot{\boldsymbol{x}}_O = \boldsymbol{0}$, $\ddot{\boldsymbol{\theta}} = \dot{\boldsymbol{\theta}} = \boldsymbol{0}$, and $\ddot{\boldsymbol{\xi}} = \dot{\boldsymbol{\xi}} = \boldsymbol{0}$, yields the linear time-invariant state equation and output equation as follows:

$$\delta\dot{\boldsymbol{z}} = \boldsymbol{A}\delta\boldsymbol{z} + \boldsymbol{B}\delta\boldsymbol{\tau} \tag{9}$$

$$\delta\boldsymbol{p} = \boldsymbol{C}\delta\boldsymbol{z} \tag{10}$$

where $\delta\boldsymbol{z} = \begin{bmatrix} \delta\boldsymbol{x}_O^T & \delta\dot{\boldsymbol{x}}_O^T \end{bmatrix}^T$ is state variables, $\delta\boldsymbol{\tau} = \boldsymbol{\tau} - \boldsymbol{\tau}_e$ is input variables and $\delta\boldsymbol{p} = \boldsymbol{p} - \boldsymbol{p}_e$ is output variables expressing the object's position and orientation. Coefficient matrices in (9) and (10) can be written by

$$\boldsymbol{A} = \begin{bmatrix} \boldsymbol{0} & \boldsymbol{I}_6 \\ -\boldsymbol{\Lambda}_O\boldsymbol{G} & \boldsymbol{0} \end{bmatrix}_{\substack{x_O=x_{Oe} \\ \theta=\theta_e \\ \xi=\xi_e}},\quad \boldsymbol{B} = \begin{bmatrix} \boldsymbol{0} \\ \boldsymbol{\Lambda}_O \end{bmatrix}_{\substack{x_O=x_{Oe} \\ \theta=\theta_e \\ \xi=\xi_e}} \tag{11}$$

$$\boldsymbol{C} = \begin{bmatrix} \boldsymbol{I}_6 & \boldsymbol{0} \end{bmatrix}$$

where the matrix $\boldsymbol{I}_6$ is a 6×6 identity matrix and $\boldsymbol{G}$ is the Jacobian matrix concerning the gravitational force $\boldsymbol{g}_{\text{sys}}$ with respect to $\boldsymbol{x}_O$.

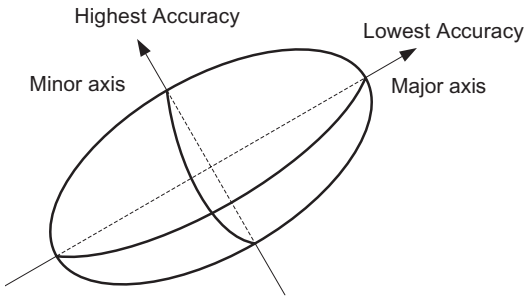

Fig. 3. Output controllability ellipsoid (OCE)

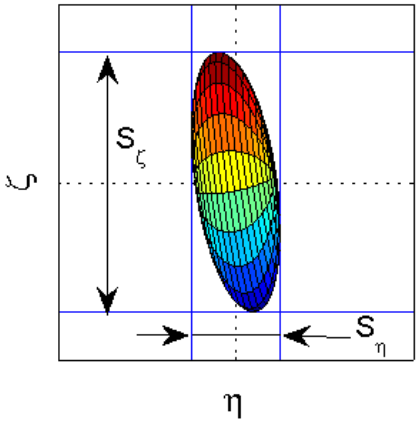

Fig. 4. Sensitivity to the direction of each coordinate axis

III. Task Accuracy Measure

A. Output Controllability Ellipsoid

A system is said to be output controllable if it is possible to construct inputs that will transfer any given initial output to any final output until a finite time [10]. When a cooperating manipulation system is output controllable, there exist joint torques which move the object to arbitrary position and orientation until a finite time. The necessary and sufficient condition for output controllable is that an output controllability matrix is non-singular. The output controllability matrix $\boldsymbol{N}$ of the cooperating manipulation system can be obtained using the matrices $\boldsymbol{A}$, $\boldsymbol{B}$ and $\boldsymbol{C}$ of (11) as follows:

$$\boldsymbol{N} = \Big[\mathbf{0} \quad \boldsymbol{\Lambda}_O \quad \mathbf{0} \quad (-\boldsymbol{\Lambda}_O \boldsymbol{G})\boldsymbol{\Lambda}_O \cdots \cdots (-\boldsymbol{\Lambda}_O \boldsymbol{G})^{11}\boldsymbol{\Lambda}_O \Big] \tag{12}$$

As seen from (12), the matrix $\boldsymbol{N}$ consists of the matrices $\boldsymbol{\Lambda}_O$ and $\boldsymbol{G}$. The output controllability depends on not only the configuration and dynamic parameters of the cooperating manipulation system but also the gravity load.

The subspace of the output-controllable object's position and orientation $\boldsymbol{p}$ steered by the input joint torque $\boldsymbol{\tau}$ is equivalent to the range space of the matrix $\boldsymbol{N}$, which is

$$\text{Range } \boldsymbol{N} = \{\boldsymbol{p} \mid \boldsymbol{p} = \boldsymbol{N}\widehat{\boldsymbol{\tau}}, \ ^{\forall}\widehat{\boldsymbol{\tau}}\} \tag{13}$$

where

$$\widehat{\boldsymbol{\tau}} = [\ \widehat{\boldsymbol{\tau}}_1^T,\ \widehat{\boldsymbol{\tau}}_2^T, \ldots,\ \widehat{\boldsymbol{\tau}}_{3n_f}^T]^T,$$
$$\widehat{\boldsymbol{\tau}}_i = \int_0^{t_f} q_i(-t)\boldsymbol{\tau}(t)dt,$$

$q_i(t)$ is some scalar function of time, and $t_f > 0$ is an arbitrary time.

The set of the output-controllable $\boldsymbol{p}$, which is realizable by the input normalized as $\widehat{\boldsymbol{\tau}}^T\widehat{\boldsymbol{\tau}} \leq 1$, forms an ellipsoid in the 6-dimensional output space, as shown in Fig. 3. The ellipsoid is referred to the Output Controllability Ellipsoid (OCE). The shape and size of the OCE reflect the characteristic of the output controllability, which can be found by the singular value decomposition of the matrix $\boldsymbol{N}$ as follows:

$$\boldsymbol{N} = \sum_{i=1}^{6} \sigma_{Ni}\boldsymbol{u}_{Ni}\boldsymbol{v}_{Ni}^T \tag{14}$$

where $\sigma_{N1} \geq \sigma_{N2} \geq \ldots \geq \sigma_{N6} > 0$ are the singular values, and $\boldsymbol{u}_{Ni}$ and $\boldsymbol{v}_{Ni}$ are corresponding singular vectors. The OCE can be described as 6-dimensional ellipsoid, which has principal axes $\sigma_{N1}\boldsymbol{u}_{N1}$, $\sigma_{N2}\boldsymbol{u}_{N2}$, ..., $\sigma_{N6}\boldsymbol{u}_{N6}$, where σ_{Ni} and $\boldsymbol{u}_{Ni}$ show the radius and direction of the ith principal axis, respectively.

The magnitudes of the singular values represent the strengths of the effects of input on output [6], [8], [13]. Therefore, when the object is steered in the direction of the major axis of the OCE shown in Fig. 3, the effect of the joint driving force (input) on the object's position and orientation (output) is maximized. Since the manipulation system has high-sensitivity in this direction, even a small input error, such as noise, greatly affects the motion of the object.

In contrast, the effect of the joint driving torque (input) on the object's position and orientation (output) is the lowest in the direction of the minor axis of the OCE. Therefore, the control accuracy is the highest since the manipulation system has low sensitivity in this direction.

In the above discussion based on the output controllability matrix $\boldsymbol{N}$ in (13), we have assumed that there is no constraint imposed on the maximum joint driving torques, $\widehat{\boldsymbol{\tau}}$, and that the weights of the components related to the translational and rotational motion of the object, $\boldsymbol{p}$, are the same. When these assumptions do not hold, normalization of inputs and/or outputs variables is needed.

B. Relative Sensitivity

In order to evaluate the task accuracy of cooperating manipulation systems quantitatively, this section proposes a performance measure obtained from the output controllability ellipsoid (OCE). As shown in Fig. 4, the length of the line segments, S_η and S_ζ, which is given by the orthographic projection of the OCE onto each η and ζ axis, implies the sensitivity to the direction of each coordinate axis. Based upon the theory of error propagation of linear systems [16], the accuracy can be determined by the sensitivity ratio between each coordinate. Thus, the relative sensitivity of the coordinate ζ to the coordinate η is defined as the task

accuracy, which is

$$S_{\zeta\eta} = \frac{S_\zeta}{S_\eta} \tag{15}$$

The task accuracy of cooperating manipulation systems is given by the sensitivity ratio between each object's coordinate. Note that the task accuracy is independent from the dimensionality since that is given by the sensitivity ratio between the object's coordinates.

C. Comparison with Conventional Manipulability

As seen from (13) and (12), the output controllable object's position and orientation (output) are determined by the joint driving forces (input) as well as the gravitational loads that are applied to the cooperating manipulation system from the past to the present. The output controllability shows a dynamic process between input and output in the system. It is required to take the dynamic process of a system into consideration in order to evaluate the control accuracy of the system [9]. Therefore, we can evaluate the task accuracy of the cooperating manipulation system by using the output controllability.

On the other hand, the conventional manipulability considers not the task accuracy but the task efficiency. For example, in the case of a cooperating manipulation system, the object's accelerations (output) for given joint torques (input) can be given by the following algebraic equation [18]

$$\ddot{\boldsymbol{x}}_O = \boldsymbol{\Lambda}_O \ \mathrm{diag}\left(1/\widetilde{\tau}_{1\,\max}, \cdots, 1/\widetilde{\tau}_{3n_f\,\max}\right)^{-1} \widehat{\boldsymbol{\tau}} \tag{16}$$

where

$$\widehat{\tau}_i = (\tau_i - g_{\mathrm{sys}i}(\boldsymbol{\theta}))/\widetilde{\tau}_{i\,\max}$$
$$\widetilde{\tau}_{i\,\max} = \tau_{i\,\max} - |g_{\mathrm{sys}i}(\boldsymbol{\theta})| > 0$$

The relationship between joint torques and object's accelerations is considered to be instantaneous. The conventional manipulability is regarded as the measure of the static process.

IV. SIMULATION EXAMPLES

In order to verify the proposed task accuracy measure, simulations are conducted by employing the robotic hand with two two-jointed fingers in a plane with grasping a circular object as shown in Fig. 5.

The physical parameters of the manipulation system are as follows: Each of the links of the finger has length l, mass m_h, and moment of inertia I_h. The mass center of each link coincides with its centroid, the distance between the first joint of the two fingers is l_b. The position and orientation of the object with radius r_O is described as $\boldsymbol{x}_O = (\ x,\ y,\ \phi\ )$, which is defined as the output variables of the manipulation system, and the mass and the moment of inertia of the object are denoted by m_O and I_O, respectively. The mass center of the object coincides with its centroid.

We assume that the fingers do not slip on the object by applying appropriate internal forces at point contacts with friction, and that the straight line connecting the both contact points crosses the mass center of the object.

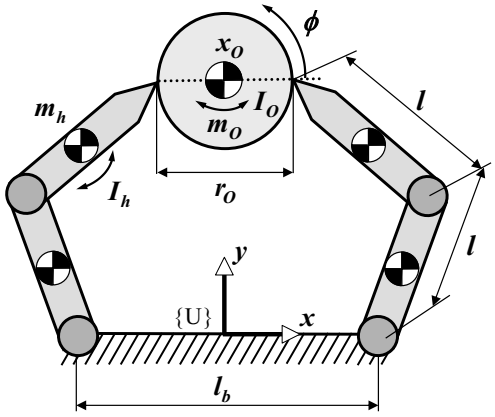

Fig. 5. The two-fingered robotic hand and its physical parameters: $m_h = 1$ kg, $I_h = 1/12$ kg $\cdot$ m^2, $l = 1$ m, $l_b = 1$m, $m_O = 5$ kg, $I_O = 5/32$ kg $\cdot$ m^2, $r_O = 0.5$ m

A. Task Accuracy

For a motion control of cooperating manipulation systems, it is desired that disturbances and modeling errors have less effect on the motion of the grasped object.

Consider a manipulation task that the robotic hand rotates the circular object by 50-degree anti-clockwise with the lateral grasp and the hook grasp [14], as shown in Figs. 6(a) and 7(a). Only the direction of gravity is different between the two grasps. The gravity is exerted in the direction of each arrowed line.

Figs. 6(b) and 7(b) show the orthographic projections of the three-dimensional output controllability ellipsoid (OCE) on the $x\phi$-plane at each object's orientation for the two grasps, respectively. These figures indicate that the difference of the direction of gravity yields a change in the shape, size and orientation of the OCE even though the robotic hand represents the same configuration.

Assuming that the robotic hand rotates the object with each lateral grasp and hook grasp, we compare the errors of the object's orientation at each final point. The desired trajectory of the object is given by the cubic polynomial of time with zero angular velocities at the initial and final time. The nominal joint torque of each grasp for the object's trajectory is obtained in advance using the equation of motion (6). The input torque is set as the sum of its nominal joint torque and the Gaussian white noise. Applying the input torque to the feedforward controller, we obtain the final position and orientation of the object. This simulation is repeated 50 times. We let the total motion time be 1.5 s, the variance of the Gaussian white noise be 25 N^{2}m^2, and the position and orientation of the object at the initial and final time be $\boldsymbol{x}_O = (\ 0,\ 1.5,\ 0\ )$ and $(\ 0,\ 1.5,\ 5\pi/18\ )$, respectively.

Figs. 8(a) and (b) show the simulation results with the lateral grasp and the hook grasp, respectively. The sign $\times$ indicates the final position and orientation of the object, and the sign $\bullet$ indicates the goal. The final orientations ϕ with the lateral grasp of Fig. 8(a) disperse from the goal. In contrast, the final orientations ϕ with the hook grasp of Fig.

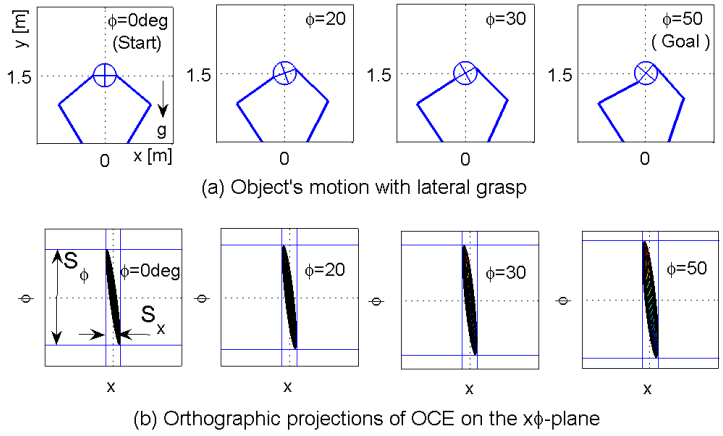

Fig. 6. Rotating the object with lateral grasp

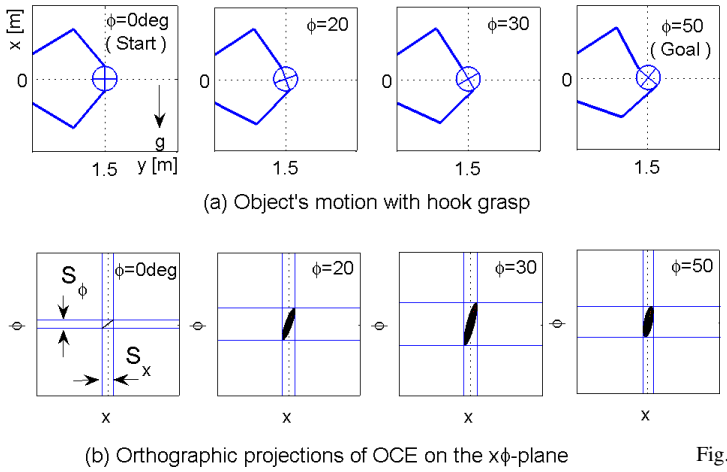

Fig. 7. Rotating the object with hook grasp

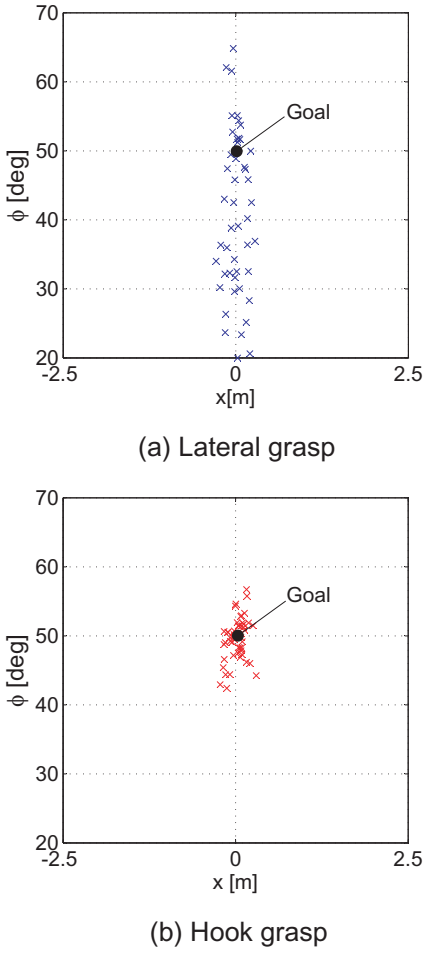

Fig. 8. Errors at final position and orientation of the object for two different grasps

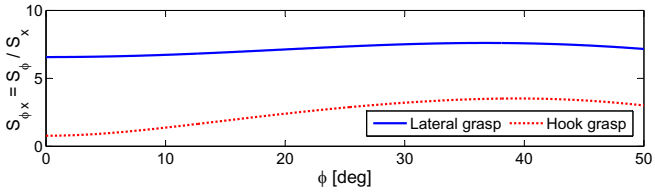

Fig. 9. Relative sensitivity $S_{\phi x}$ of two different grasps with gravity

8(b) converge in the neighborhood of the desired orientation. These results indicate that the manipulation with the hook grasp is more accurate than that with the lateral grasp.

As mentioned in section III-B, the difference in task accuracy arises from the difference in the relative sensitivity of the lateral grasp and the hook grasp. Let S_x and S_ϕ denote the sensitivity in direction of the x and ϕ axes, respectively, as shown in Figs. 6 (b) and 7 (b). The relative sensitivity of the orientation ϕ to the position x can be given by $S_{\phi x} = S_\phi / S_x$. If the value of $S_{\phi x}$ becomes larger, then the manipulation system becomes more sensitive for the object's orientation. Therefore, the task accuracy of the manipulation becomes lower for the orientation. In contrast, if the value of $S_{\phi x}$ becomes smaller, then the manipulation system becomes less sensitive for the object's orientation. Therefore, the task accuracy of the manipulation becomes higher for the orientation.

The relative sensitivity $S_{\phi x}$ with the lateral grasp and the hook grasp are shown in Fig. 9. This figure shows that the value of $S_{\phi x}$ with the hook grasp is smaller than that with the lateral grasp through the rotational manipulation. This means that the hook grasp is less sensitive and higher accurate for the rotational manipulation than the lateral grasp. This result corresponds to the simulation results of the final errors shown in Fig. 8.

Finally, we consider the effect of a gravity for the task accuracy. Fig. 10(a) shows orthographic projections of the OCE for the same manipulation task shown in Figs. 6 and 7 without taking the gravitational effect into the consideration. The size, shape and orientation of the OCE with two grasps totally coincide through the manipulation. The relative sensitivity $S_{\phi x}$ of the two grasps also have the identical value as shown in Fig. 10(b). This means that the task accuracy for a manipulation system with the same grasp

configuration becomes identical when a gravity is not taken into consideration.

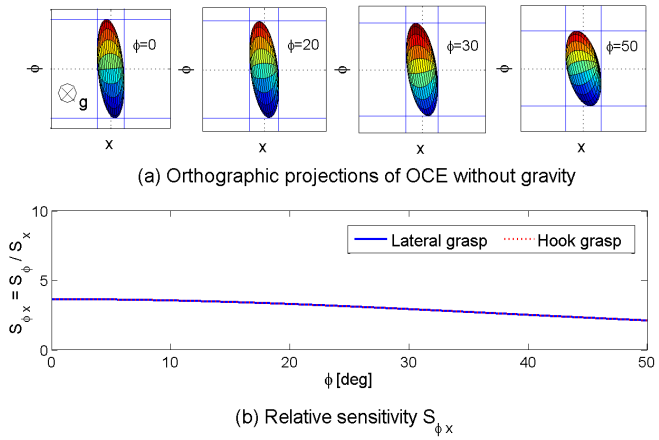

Fig. 10. Manipulation performance of two different grasps without gravity

B. Comparison with Conventional Manipulability

Fig. 11 (a) and (b) show the orthographic projections of the output controllability ellipsoid (OCE) and the dynamic manipulability ellipsoid (DME) on the xy-plane with/without gravitational effect, respectively. When the gravitational effect is considered, their size, shape and orientation are totally different. In contrast, when the gravitational effect is not considered, the OCE and the DME are identical as shown in Fig. 11(b). This result indicates that the DME shows the task accuracy as well as the task efficiency only without gravitational effect.

V. CONCLUSION

The present paper proposed the task accuracy measure for cooperating manipulation system with taking its dynamic process into consideration. We are now planning to conduct experiments in order to show the validity of the task accuracy measure for a real cooperating manipulation system.

The proposed measure can be applied to various types of robots since the measure is based on the linear system theory. In the future, the applicability of the measure shall be extended to robotic systems that have complicated constraints, such as friction or non-holonomic constraints. We will also consider task-oriented manipulation by using the task accuracy measure.

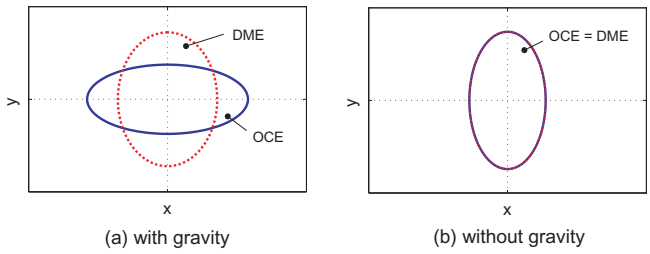

Fig. 11. Output controllability ellipsoid (OCE) and dynamic manipulability ellipsoid (DME) at $\boldsymbol{x}_O = [\ 0\ \ 1.2\ \ 0\ ]^T$ ($\tau_{max} = 100$Nm for DME)

REFERENCES

[1] H. Asada, "A geometrical representation of menipulator dynamics and its application to arm design," Trans. of ASME, J. Dynamics Systems, Measuremet and Control, vol.105, no.3, pp.131-135, 1983.

[2] A. Bicchi, C. Melchiorri, and D. Balluchi, "On the mobility and manipulability of general multiple limb robots," IEEE Trans. on Robotics and Automation, vol.11, no.2, pp.215-228, 1995.

[3] P. Chiacchio, S. Chiaverini, L. Sciavicco and B. Siciliano, "Global task manipulability ellipsoids for multiple-arm systems," IEEE Trans. on Robotics and Automation, vol.7, no.5, pp.678-685, 1991.

[4] P. Chiacchio, S. Chiaverini, L. Sciavicco and B. Siciliano, "Task space dynamic analysis of multiarm system configurations," The Int. J. of Robotics Research, vol.10, no.6, pp.708-715, 1991.

[5] S.L. Chiu, "Task compatibility of manipulator postures," The Int. J. of Robotics Research, vol.7, no.5, pp.13-21, 1988.

[6] B. Friedland, "Controllability index based on conditioning number," Trans. of ASME, J. Dynamics Systems, Measuremet and Control, pp.444-445, December 1975.

[7] T. J. Graettinger and B. H. Krogh, "The acceleration radius: a global performance measure for robotic manipulators," IEEE J. of Robotics and Automation, vol.4, no.1, pp.60-69, 1988.

[8] C. D. Johnson, "Optimization of a certain quality of complete controllability and observability for Linear Dynamical Systems," Trans. of ASME, J. Basic Engineering, pp.228-238, June 1969.

[9] T. Kailath, "Linear systems," Prentice-Hall Inc., 1980.

[10] E. Kreindler and P. E. Sarachik, "On the concepts of controllability and observability of linear systems," IEEE Trans. on Automatic Control, vol.9, no.2, pp.129-136, 1964.

[11] O. Ma and J. Angeles, "Optimal design of manipulators under dynamic isotropy conditions," Proc. IEEE Int. Conf. on Robotics and Automation, pp.2424-2429, 1993.

[12] D. J. Montana, "The kinematics of contact and grasp," The Int. J. of Robotics Research, vol.7, no.3, pp.174-32, 1988.

[13] B. C. Moore, "Principal component analysis in linear systems: controllability, observability and model reduction," IEEE Trans. Automatic Control, vol.26, no.1, pp.17-32, 1981.

[14] P.J. Rash and R.K. Burke, "Kinesiology and applied anatomy," Lea & Febiger, 1974.

[15] J. K. Salisbury and J. J. Craig, "Articulated hands: force control and kinematic issues," The Int. J. of Robotics Research, vol.1, no.1, pp.4-17, 1982.

[16] G. Strang, "Linear algebra and its application, third edition," Thomson Learing, 1988.

[17] T. Yoshikawa, "Manipulability of robotic mechanisms," The Int. J. of Robotics Research, vol.4, no.1, pp.3-9, 1985.

[18] T. Yoshikawa, "Dynamic manipulability of robotic mechanism," J. Robotic Systems, vol.2, no.1, pp.113-124, 1985.